RECENT DEVELOPMENTS TOWARDS THE SDLS*

D. Khan†, X. Huang, P. Liu, Y. Nosochkov, J. Safranek,
SLAC National Accelerator Laboratory, Menlo Park, United States

Abstract

We report on the development of an advanced storage ring lattice, the Stanford Diffraction-Limited Light Source, tailored for installation in the existing PEP-II tunnel at SLAC, which consists of six arcs and six long straight sections. The SDLS cell is based on the hybrid 6-bend achromat optics optimized for ultra-low emittance and maximum dynamic aperture, essential for diffraction-limited synchrotron radiation production. The long straight sections, which will house the insertion devices and injection systems, are designed to satisfy the transparency conditions that mitigate periodicity-breaking effects affecting the dynamic aperture and momentum acceptance. The latest designs advances the SDLS concept by replacing the H6BA cell with a non-achromatic cell or combining a new compact (insertion device-less) cell in three arcs and the H6BA in the other arcs.

INTRODUCTION

The Stanford Synchrotron Radiation Lightsource (SSRL) is a third-generation synchrotron light source facility currently operating the Stanford Positron–Electron Asymmetric Ring-III (SPEAR3) [1]. It has served as a major facility for photon science and accelerator research, but recent advances in accelerator physics and magnet technology have driven the global development of next-generation diffraction-limited storage rings. To maintain SSRL's competitiveness among modern synchrotron facilities, multiple upgrade strategies have been investigated. One such upgrade, the Stanford Diffraction Limited Synchrotron (SDLS), involves the construction of a storage ring equipped with Hybrid Six-Bend Achromat cells (H6BA) [2] within the existing Positron Electron Project (PEP) tunnel. The PEP tunnel features a six-fold symmetric geometry consisting of six arcs, each 243.2 m, and six long straight sections (SS), each 123.35 m, giving a total ring circumference of 2199.3 m.

The H6BA cell (Fig. 1, left), recently proposed as a promising architecture for diffraction-limited storage rings [3], serves as the foundation of the upgrade discussed here. The design prioritizes maximizing the photon beam brightness while simultaneously ensuring operational performance through large dynamic aperture (DA), high momentum acceptance (MA), off-axis injection capability, and long beam lifetime. These performance goals are intended to reduce the demands on the injector system while maintaining robust long-term beam storage. Additionally, transparency conditions are also implemented in the long SS optics to preserve favorable nonlinear beam dynamics (Fig. 2, left).

* Work supported by the U.S. DOE Contract DE-AC02-76SF00515.
† donish@slac.stanford.edu

Since the PEP tunnel is underground, excavation is required to create space for photon beamlines. On-site surveying has determined that three arcs are suitable for excavation and beamline construction while the other three arcs will be deemed vacant [4]. Under these constraints, at least 33 insertion device (ID) beamlines can be accommodated in short-ID SS, with six additional beamlines possible in adjacent long SS. The vacant arcs give flexibility in optics design and an opportunity to further push the limits of performance.

In this paper, we present two non-achromatic variations of the SDLS's nominal H6BA cell, currently under development. The first is the H6BN cell, retaining much of the nominal H6BA's characteristics but with reduced emittance. The second is an emittance-minimized, compact cell, the CH6B, that is intended only for the three vacant arcs while the H6BA will be used in the other arcs. In the next sections, the methodology for these alternative designs is outlined, and the overall performance is compared with that of the SDLS's nominal H6BA at 5 GeV electron energy.

ALTERNATIVE LATTICE DESIGNS

All designs assumed the use of experimentally demonstrated technologies, including conventional magnet and vacuum system [5]. Combined-function dipoles with longitudinal field gradients are utilized to improve emittance performance and increase lattice compactness. The dipoles include integrated quadrupole field to provide distributed focusing while maintaining the required bending profile. Quadrupole gradients were limited to 110 T/m, consistent with state-of-the-art magnet technology. A summary of the cell optical parameters is listed in Table 1.

Table 1: Parameters of H6BA, H6BN, and CH6B cells

Parameter	Units	H6BA	H6BN	C6HB
ϵ_x	pm rad	28	18	13
Q_x	–	1.77	1.77	1.41
Q_y	–	0.91	0.91	0.61
Nat. ξ_x	–	-2.6	-2.5	-2.5
Nat. ξ_y	–	-2.9	-2.9	-4.7
σ_E/E_0	10^{-4}	6.4	8.0	6.1
$U_0/Cell$	keV	9.5	11.9	5.7
J_x	–	1.67	1.60	1.96
α_c	10^{-5}	3.93	3.73	4.03

H6BN

The H6BN cell was developed as a direct replacement for the H6BA cell across all arcs, hence twelve H6BN cells can be included per arc. This cell (Fig. 1, middle) is designed to reduce the H6BA's emittance by optimizing the

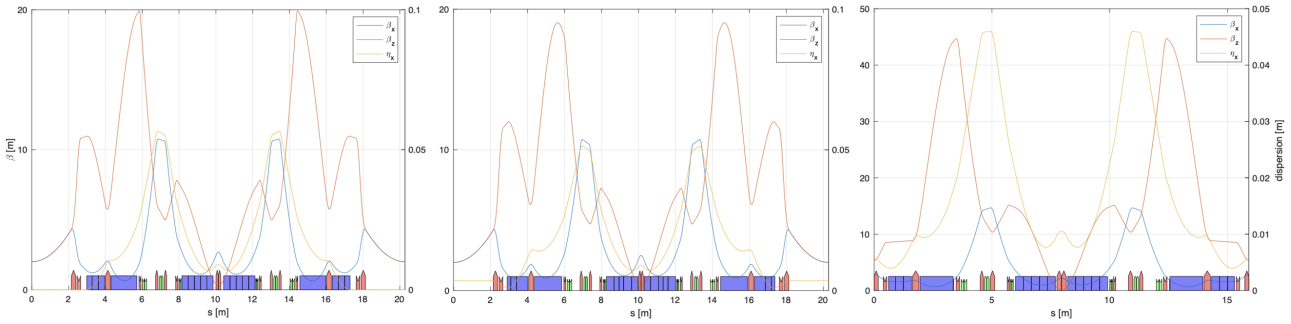

Figure 1: Optical functions for the different cell configurations: (left) nominal H6BA cell, (middle) H6BN cell, and (right) CH6B cell. For each plot, the left y-axis represents the betatron amplitude, while the right y-axis represents the dispersion.

dispersion function's profile within the dipoles. This requires a small dispersion leakage in the short-ID SS, which will affect the photon brightness via $\mathcal{B} \propto 1/\epsilon_x \sqrt{1 + \frac{(\eta \sigma_E)^2}{\beta_x \epsilon_x}}$. Using 1-dimensional scans, an approximate optimal configuration that balances brightness, ID dispersion (3.5 mm), and emittance (18 pm) was found.

CH6B

The CH6B cell (Fig. 1, right) was designed for the vacant arcs and to maximally reduce the emittance. Under this configuration, three arcs of the nominal H6BA lattice would be replaced with CH6B cells. As a first step, we discarded the short-ID SS thereby reducing the cell's length and bending angle by a factor of 12/15, hence fifteen CH6B cells can be included per arc. A significant modification of the dispersion function profile was carried out, with the dispersion waists minimized and symmetrically repositioned within each dipole. The change in the bending profile results in a significant reduction of the curly $\mathcal{H}$ function within the cell yielding 13 pm natural emittance.

Design Considerations

Several constraints were imposed on the design of the new lattice configurations. First, the ring fractional tunes were selected from the nominal SDLS's value of 0.2 in both planes [2]. This working point is far from integer and half-integer resonances, thus suppressing the corresponding resonance effects. On the other hand, it is at a coupling resonance which simplifies implementation of a round beam. The long SS (Fig. 2) were initially designed to satisfy the original transparency conditions [3]. However, due to periodicity breaking in a ring with different types of arc optics, enforcement of the transparency conditions was relaxed for the lattice with CH6B and H6BA arcs. To nullify dispersion in the SS, dispersion suppressors were required for both the new cells. The suppressors are based on the regular cells optimized for low emittance while canceling the linear dispersion as well as providing the optimal second order dispersion.

Matching of the linear optics (Twiss parameters), chromatic functions (Montague W-functions, second-order dispersion), and the phase advance in the long SS according to the transparency conditions was performed for suppression of systematic resonance effects [3]. The second-order dispersion in the SS presented a considerable challenge, particularly between the H6BA and CH6B arcs, due to the limited tuning in the dispersion suppressor, as well as no dispersion or higher-order magnets in the SS. Furthermore, the match of chromatic functions in the SS is sensitive to change of sextupole strengths in the arcs; therefore, tuning of the sextupole strengths in the arcs introduce small but non-negligible chromatic mismatches that propagate through the lattice. Lastly, each lattice was configured with a net chromaticity of +5 in both planes suitable for collective instability suppression.

SIMULATION RESULTS

The optics design and matching was performed with a combination of MAD8 [6], Bmad [7], and AT [8] whereas, particle tracking for dynamic aperture (DA), local momentum aperture (LMA), and tune shift with energy deviation were performed using AT.

The DA (Fig. 3) for on-energy tracking shows notable variation between the H6BA and new lattices. Both alternative lattices result in a reduction in overall DA area, where the CH6B experiences the most significant degradation. This reduction is likely associated with the breaking of periodicity in the CH6B arc-configuration, which weakens the cancellation of nonlinear driving terms that would otherwise be reinforced by symmetry. As a result, resonance driving terms accumulate more strongly over successive cells, leading to a reduced stable region in phase space and therefore a smaller DA. Table 2 shows the higher-order magnet strengths for each lattice.

Table 2: Sextupole and octupole family strengths for H6BA, H6BN, and CH6B lattices.

	Units	**H6BA**	**H6BN**	**CH6B**
K_{SD1}	m^{-3}	-220	–	-224
K_{SF1}	m^{-3}	221	–	230
K_{SD2}	m^{-3}	-220	–	-236
K_{SD3}	m^{-3}	–	-256	-258
K_{SF2}	m^{-3}	–	267	186
K_{SD4}	m^{-3}	–	-256	-176
K_{OCT1}	m^{-4}	-16200	-20200	-16200
K_{OCT2}	m^{-4}	–	–	-4900

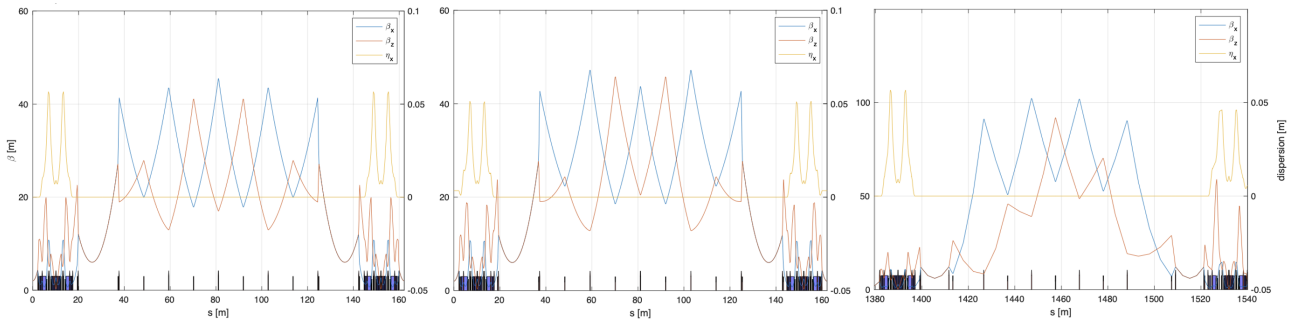

Figure 2: Straight-section optics for different matching configurations: (left) H6BA-to-H6BA matching, (middle) H6BN-to-H6BN matching, and (right) H6BA-to-CH6B matching. For each plot, the left y-axis represents the betatron amplitude, while the right y-axis represents the dispersion.

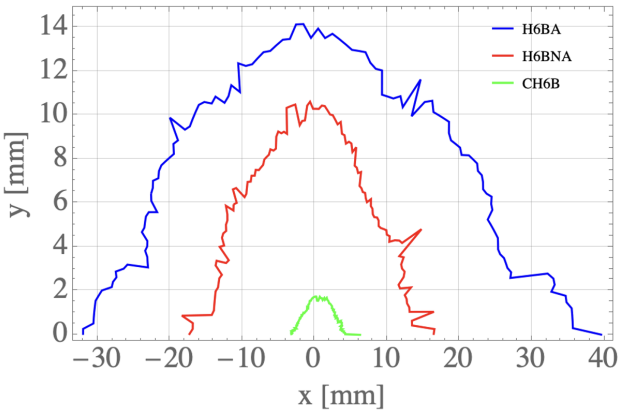

Figure 3: On-energy ($\delta_p = 0$) dynamic aperture for each lattice configuration evaluated at $\beta_x = 45.5$ m and $\beta_y = 17$ m.

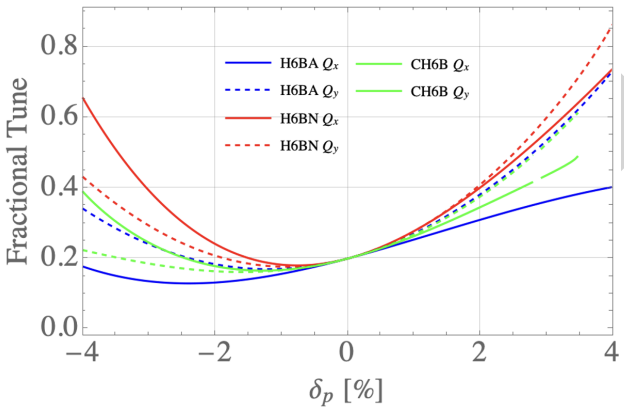

Figure 4: Tune shift with energy deviation for each lattice configuration.

Figure 4 shows the tune shift as a function of energy deviation for each lattice. The fractional tune crosses the half-integer resonance at approximately +3% for H6BN in Q_x and for all lattices in Q_y, and at approximately −3% for H6BN in Q_x. Instability occurs at the half-integer resonance, where particles are lost during tracking; an artifact of this effect is visible in the CH6B case (dashed and solid green).

The three lattices exhibit clearly distinct LMA profiles. The H6BA lattice (blue) provides the largest momentum acceptance overall, with the positive aperture remaining close to +4% over most of the cell and its negative aperture typically around -5%. The H6BN lattice (red) shows an intermediate acceptance profile. The positive aperture remains near +3% across the cell, with a modest rise toward +4.5% around the center and at the cell boundaries. The negative aperture stays close to -3.5% over much of the lattice, with localized reductions reaching roughly -6%. The CH6B lattice (green) exhibits the smallest overall momentum acceptance range. Both it's positive and negative aperture is comparatively uniform, staying near +2.5% to +3% throughout the cell with only minor local fluctuations. This comparatively flat and symmetric profile indicates much weaker longitudinal variation in off-momentum acceptance than in the H6BA and H6BN cases.

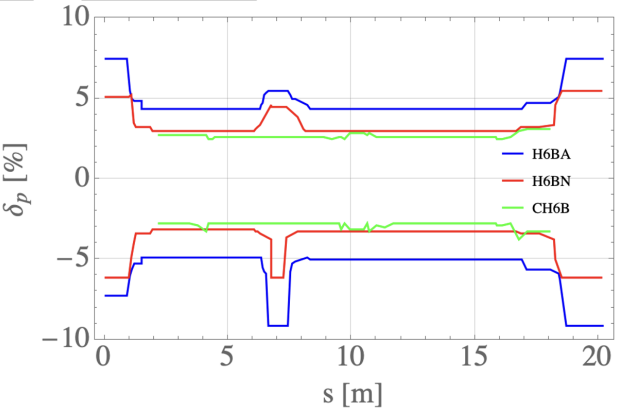

Figure 5: The local momentum aperture across each cell.

FUTURE DEVELOPMENTS

Future work will focus on full-lattice nonlinear beam dynamics optimization using multi-objective evolutionary algorithms. These studies aim to further enhance the DA, MA, and Touschek lifetime. Additional optimization studies will investigate the impact of different positive chromaticity settings on ring performance and in parallel, continued exploration of linear optics design will be carried out to further push lattice performance.

REFERENCES

[1] R. Hettel *et al.*, "The Completion of SPEAR 3", in *Proc. EPAC'04*, Lucerne, Switzerland, Jul. 2004, paper THPKF082, pp. 2451–2453.

[2] P. Raimondi, X. Huang, J. Kim, J. Safranek, and T. Rabedeau, "Advanced storage ring lattice options based on hybrid six-bend achromat for Stanford Synchrotron Radiation Lightsource upgrade", *Nucl. Instrum. Methods Phys. Res. A*, vol. 1061, p. 169137, 2024. doi:10.1016/j.nima.2024.169137

[3] P. Raimondi and S. M. Liuzzo, "Toward a diffraction limited light source", *Phys. Rev. Accel. Beams*, vol. 26, no. 2, p. 021601, 2023. doi:10.1103/PhysRevAccelBeams.26.021601

[4] SLAC National Accelerator Laboratory, "PEP-X Light Source at SLAC — Status Report, Revision 0", USA, SLAC Report, June 10, 2008.

[5] J. Biasci *et al.*, "A low-emittance lattice for the ESRF", *Synchrotron Radiat. News*, vol. 27, no. 6, pp. 8–12, 2014. doi:10.1080/08940886.2014.970931

[6] F. Schmidt, "MAD program (MAD8), User's Reference Manual", CERN, Geneva, Switzerland, CERN/SL/94-97 (AP),1994.

[7] D. Sagan, "Bmad: A relativistic charged particle simulation library", *Nucl. Instrum. Methods Phys. Res. A*, vol. 558, pp. 356–359, 2006. doi:10.1016/j.nima.2005.11.001

[8] A. Terebilo, "Accelerator Modeling with MATLAB Accelerator Toolbox", in *Proc. PAC'01*, Chicago, IL, USA, Jun. 2001, paper RPAH314, pp. 3203–3205.